Analysis of an Automatically Tuned Filter and its Application at Microwave Frequencies

Eckhard Neber[1], Sébastien Quintanel[2], Laurent Billonnet[2], Bernard Jarry[2], Michael H.W. Hoffmann[1]

[1] University of Ulm, Albert-Einstein-Allee 41, 89081 Ulm, Germany
Tel: +49 731 5026354, Email: neber@mwt.e-technik.uni-ulm.de
[2] IRCOM UMR C.N.R.S. 6615, 123 Avenue Albert Thomas, 87060 Limoges Cédex, France
Tel: +33 555457254, Email: gary@ircom.unilim.fr

***Abstract* — This paper analyses an automatically tuned filter and its application at microwave frequencies in detail. The filter is implemented in a master-slave structure. Either the phase or the magnitude response of the master-filter at a reference frequency is used to find information on potential operating points and on the stability of the complete control structure. The theory is simulated and compared to measured results.**

I. Introduction

The characteristics of analog filters are vulnerable to fabrication tolerances and temperature drift. Automatic frequency control using the popular master-slave approach is the most feasible solution to control these characteristics [1]. It uses a master device that is embedded in a control loop to generate the tuning signal for the slave *Voltage Controlled Filter (VCF)* in the signal path (cp. Fig. 1). A good matching between master and slave is essential for a precise operation.

For microwave filters, this problem has been solved in [2], [3] by using a typical phase locked loop based on a voltage controlled oscillator matched to the slave filter.

Another control scheme that uses identical filters for master and slave was proposed in [4]. It utilises a test signal to measure either the magnitude response (*Magnitude Controlled Filter, MCF*) or the phase response (*Phase Controlled Filter, PCF*) of the filter at a reference frequency.

The analysis of the latter systems concentrated on transient simulations for an initial condition and a steady-state analysis. In this paper an advanced analysis is proposed that uses a linearisation in the steady-state to derive a transfer function of the system as well as information about the stability of the system.

In the first part of the paper a theoretical analysis of the control structure is given, using a generalised representation for the detector that allows it to treat the MCF as well as the PCF in the same manner. Models for the system components are introduced to illustrate the procedure. In the second part, the theory is applied to a band pass filter with variable centre frequency in an MCF and a PCF system. The results are validated by measurements with a PCF system at microwave frequencies.

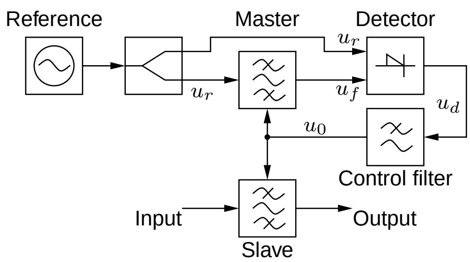

Fig. 1. Principle structure of the control loop.

II. Theoretical analysis

The structure of an automatically tuned filter following the master–slave principle is shown in Fig. 1. The sinusoidal reference signal $u_r(t) = \hat{u}_r \cos(\omega_r t)$ with angular frequency ω_r is applied to the master filter as well as to a detector. The behaviour of the master filter with centre angular frequency ω_0 is described by the transfer function $H(p, \omega_0)$. A second order band pass transfer function will be used in the examples:

$$H(p, \omega_0) = \frac{H_0 \dfrac{p}{\omega_0 Q_0}}{1 + \dfrac{p}{\omega_0 Q_0} + \dfrac{p^2}{\omega_0^2}} \tag{1}$$

with H_0 being the gain at centre frequency, $Q_0 = {}^{\omega_0}/_{\Delta\omega_0}$ and $\Delta\omega_0$ (in ${}^{\mathrm{rad}}/_{\mathrm{s}}$) the angular frequency bandwidth at -3 dB. The relation between the centre angular frequency and the tuning voltage is given by $\omega_0(t) = \omega_{0,0} + k_f u_0(t)$ with the VCF conversion factor k_f (in ${}^{\mathrm{rad}}/_{\mathrm{s\,V}}$) and the quiescent angular frequency $\omega_{0,0}$.

The detector might either be sensitive to the peak voltages of the input signals only (MCF, Fig. 2(a)) or to their phase difference (PCF, Fig. 2(b)). For a general analysis, the output signal of the concatenation of the power splitter, the master filter and the detector is described by a function $u_d(t) = g(\omega_r, \omega_0, \hat{u}_r)$. For the MCF the output signal is proportional to the power difference of

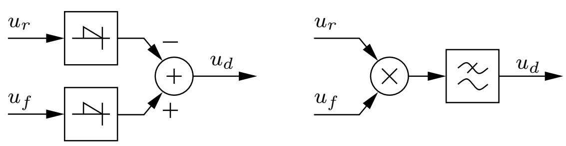

(a) Magnitude detector

(b) Phase detector

Fig. 2. Principle structure of the detector circuits. The nonlinear blocks in (a) represent power detectors.

the incoming signal $u_d(t) = k_p(\hat{u}_f^2 - \hat{u}_r^2)$, with k_p in V^{-1}. Together with (1) the nonlinear function of the MCF is:

$$g(\omega_r, \omega_0, \hat{u}_r) = -k_p \hat{u}_r^2 \frac{1 - H_0^2 + Q_0^2 \left(\frac{\omega_0}{\omega_r} - \frac{\omega_r}{\omega_0}\right)^2}{1 + Q_0^2 \left(\frac{\omega_0}{\omega_r} - \frac{\omega_r}{\omega_0}\right)^2} . \tag{2}$$

For the PCF with the detector following Fig. 2(b) it is:

$$g(\omega_r, \omega_0, \hat{u}_r) = -\frac{1}{2} k_m \hat{u}_r^2 H_0 \frac{Q_0 \left(\frac{\omega_0}{\omega_r} - \frac{\omega_r}{\omega_0}\right)}{1 + Q_0^2 \left(\frac{\omega_0}{\omega_r} - \frac{\omega_r}{\omega_0}\right)^2} \tag{3}$$

with k_m (in V^{-1}) being a constant of the multiplier.

The *Control Filter (CF)* in the feedback path is typically a low pass filter together with an amplifier. In the analysis it is represented by its impulse response $h_{\mathrm{CF}}(t)$ or its Laplace transform, the transfer function $H_{\mathrm{CF}}(p)$. Thus

$$u_0(t) = \int_{-0}^{t+0} h_{\mathrm{CF}}(t-\tau) u_d(\tau) \mathrm{d}\tau + u_{0,0}(t) \tag{4}$$

with $u_{0,0}(t)$ considering settling effects due to initial conditions in the control filter. With $u_C(0)$ being the initial voltage of the capacitor, a first order low pass filter yields:

$$H_{\mathrm{CF}}(p) = \frac{A}{1 + pRC} , \quad u_{0,0}(t) = u_C(0) \, \mathrm{e}^{-t/RC} . \tag{5}$$

The control system adjusts the centre angular frequency ω_0 of the filter to the reference angular frequency ω_r. Its behaviour is described by the integral equation:

$$\begin{aligned} \omega_0(t) = k_f \int_{-0}^{t+0} h_{\mathrm{CF}}(t-\tau) g\left(\omega_r(\tau), \omega_0(\tau), \hat{u}_r(\tau)\right) \mathrm{d}\tau \\ + \omega_{0,0} + k_f u_{0,0}(t) . \end{aligned} \tag{6}$$

Due to the nonlinearity represented by $g()$, the equation cannot be solved analytically in general. To gain insight into the structural behaviour of the system, we will apply the methods of steady-state solutions and linearisation that are also successfully used in the analysis of phase locked loops [5]–[7].

Provided that the angular frequency and the amplitude of the reference signal are constant, the centre angular frequency of the VCF will settle at a constant value. In terms of the system equation (6) this is equivalent to a steady-state solution. These stationary solutions are called *Operating Points (OP)*. The conditional equation for the OP might be derived from (6) for $(\omega_r,\ \omega_0,\ \hat{u}_r) = \text{const.}$:

$$\omega_0 = \omega_{0,0} + k_f \left(\lim_{t\to\infty} u_{0,0}(t) + H_{\mathrm{CF}}(0) g(\omega_r, \omega_0, \hat{u}_r) \right) . \tag{7}$$

$H_{\mathrm{CF}}(0)$ is the DC-gain of the control filter. The limit of the control filter transient term usually tends to zero.

The OPs might be considered as equilibrium points of the system. However, the analysis does not provide any information, whether the equilibrium is stable or unstable. An OP is stable if the system returns to this point after a slight perturbation, otherwise it is unstable.

For the stability analysis, the nonlinear function $g()$ of the system is expanded into a linear Taylor series at the OP:

$$g(\omega_r, \omega_0, \hat{u}_r) \approx u_{d,0} + K_d \omega_0 + K_r \Delta\omega_r + K_u \Delta\hat{u}_r \tag{8}$$

with

$$K_d = \left.\frac{\partial g}{\partial \omega_0}\right|_{\mathrm{OP}} , \quad K_r = \left.\frac{\partial g}{\partial \omega_r}\right|_{\mathrm{OP}} , \quad K_u = \left.\frac{\partial g}{\partial \hat{u}_r}\right|_{\mathrm{OP}} , \tag{9}$$

$$\Delta\omega_r = \omega_r - \omega_{r,\mathrm{OP}} , \qquad \Delta\hat{u}_r = \hat{u}_r - \hat{u}_{r,\mathrm{OP}} , \tag{10}$$

$$u_{d,0} = g(\omega_r, \omega_0, \hat{u}_r)|_{\mathrm{OP}} - K_d \omega_{0,\mathrm{OP}} . \tag{11}$$

The integral equation is linearised and Laplace transformed:

$$\begin{aligned} \omega_0(p) = \left[\frac{u_{d,0}}{p} + K_u \Delta\hat{u}_r(p) + K_r \Delta\omega_r(p) \right] \frac{H(p)}{K_d} \\ + \left[\frac{\omega_{0,0}}{p} + k_f u_{0,0}(p) \right] (1 + H(p)) \end{aligned} \tag{12}$$

with

$$H(p) = \frac{k_f K_d H_{\mathrm{CF}}(p)}{1 - k_f K_d H_{\mathrm{CF}}(p)} . \tag{13}$$

For the operating point, it was assumed that the system is settled in a steady-state. Therefore, it is reasonable to neglect all terms in the equation above that vanish as $t \to \infty$. Together with the formula for the operating points (7) it is then rewritten as:

$$\omega_0(p) = \frac{\omega_{0,\mathrm{OP}}}{p} + H(p) \left[\frac{K_r}{K_d} \Delta\omega_r(p) + \frac{K_u}{K_d} \Delta\hat{u}_r(p) \right] \tag{14}$$

to describe the system behaviour for small disturbances from the OP. The well-known methods of system theory might be used to analyse the stability of each OP [8] that is determined by the stability of $H(p)$ for steady-state input signals.

For the control filter used in the example it is:

$$H(p) = \frac{A k_f K_d}{1 - A k_f K_d + pRC} . \tag{15}$$

To obtain a stable system the only pole of $H(p)$:

$$p = \frac{A k_f K_d - 1}{RC} \tag{16}$$

must be located in the left half of the complex plane.

Apart from the stability considerations, the linearised equation (14) might be used to investigate the system response on perturbations like a step or a ramp of the reference frequency, as long as they are sufficiently small.

III. Results

For the solution of the OP equation (7), two methods will be carried out. The first graphical method is suitable to gain insight into the structural behaviour of the solution, whereas the second numerical solving might be easily automated with a computer. The system parameters are chosen to form an instructive example and to be comparable to the measurements of the realised system.

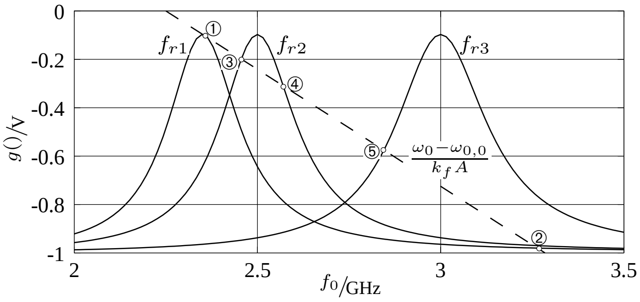

Fig. 3. Graphical solutions of the MCF system in the steady-state for the parameters: $f_0 = {}^{\omega_0}/_{2\pi}$, $f_r = {}^{\omega_r}/_{2\pi}$, $f_{r1} = 2.35\,\mathrm{GHz}$, $f_{r2} = 2.5\,\mathrm{GHz}$, $f_{r3} = 3\,\mathrm{GHz}$, $H_0 = 0.95$, $Q_0 = 10$, $\omega_{0,0} = 2\pi \cdot 2.25\,\mathrm{GHz}$, $A = -5$, $k_f = 1.3 \cdot 10^9\,{}^{\mathrm{rad}}/_{\mathrm{V\,s}}$, $k_p \hat{u}_r^2 = 1\,\mathrm{V}$.

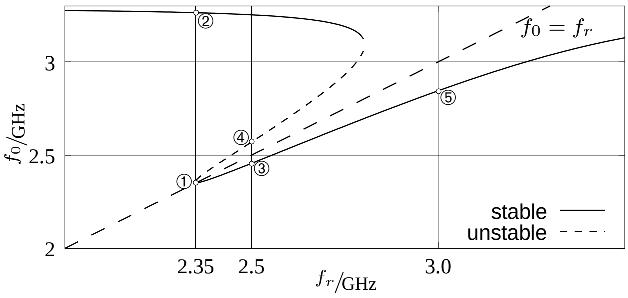

Fig. 4. Numerical solution of the MCF system in the steady-state for the same parameters as in Fig. 3.

A. Magnitude Controlled Filter

The conditional equation for the OP is rewritten as

$$g(\omega_r, \omega_0, \hat{u}_r) = \frac{\omega_0 - \omega_{0,0}}{k_f A}\,. \tag{17}$$

Fig. 3 shows a plot of the right- (dashed line) and the left-hand side (solid line) of the equation for different reference frequencies. The intersections are the OP of the MCF. It can be seen that for $f_r < f_{r1}$ there is only one intersection (②) that leads to an unusable centre frequency of the filter. For higher frequencies (f_{r2}) there are three intersections, where two of them (③, ④) lead to a centre frequency with a moderate frequency deviation from the reference. For even higher f_r there occurs only one OP as shown for f_{r3}.

The graphical method is not well suited for stability considerations since it requires to determine K_d as the slope of the tangent in the considered OP.

A numerical analysis of the conditional equations for the OP and stability were done in a range of reference frequencies using the computer algebra system *Maple 8*. Fig. 4 shows the result as a plot of the centre frequency of the OP vs. reference. The intersections from the graphical analysis are indicated as well. It turns out that for curves with two usable OPs (e.g. $f_{r2} = 2.5\,\mathrm{GHz}$, ③, ④) always one of them is unstable. The third OP is also stable, i.e. the initial conditions decide, which steady-state is reached. This is an undesirable situation for a control system. For higher reference frequencies (e.g. $f_{r3} = 3\,\mathrm{GHz}$), there exists only one stable operating point but it leads to a larger frequency error.

Hence, for an MCF control system it is not possible to combine high accuracy with only one stable operating

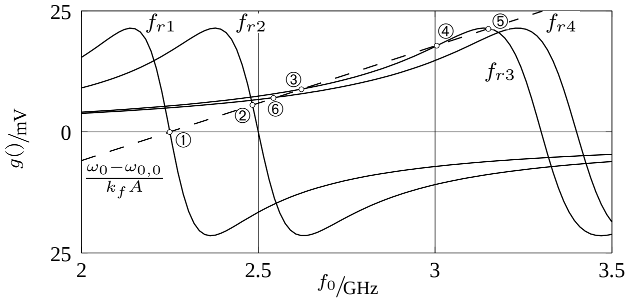

Fig. 5. Graphical solutions of the PCF system in the steady-state for the following parameters: $f_0 = {}^{\omega_0}/_{2\pi}$, $f_r = {}^{\omega_r}/_{2\pi}$, $f_{r1} = 2.25\,\mathrm{GHz}$, $f_{r2} = 2.5\,\mathrm{GHz}$, $f_{r3} = 3.3\,\mathrm{GHz}$, $f_{r4} = 3.4\,\mathrm{GHz}$, $H_0 = 0.66$, $Q_0 = 10$, $\omega_{0,0} = 2\pi \cdot 2.25\,\mathrm{GHz}$, $A = 200$, $k_f = 1.3 \cdot 10^9\,{}^{\mathrm{rad}}/_{\mathrm{V\,s}}$, $k_m \hat{u}_r^2 = 0.13\,\mathrm{V}$.

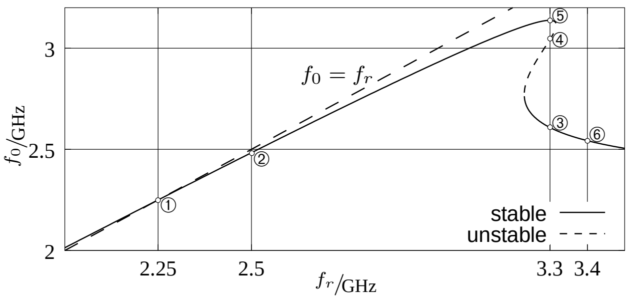

Fig. 6. Numerical solution of the PCF system in the steady-state for the same parameters as in Fig. 5.

point.

B. Phase Controlled Filter

The same analysis was carried out for a PCF system as well. The result of the graphical analysis is depicted in Fig. 5. For lower reference frequencies (e.g. f_{r1}, f_{r2}) there is only one intersection of the curves (①, ②), hence, there is only one OP. The numerical analysis (Fig. 6) shows, that it is stable. Furthermore, the accuracy is very good.

For larger reference frequencies (f_{r4}) there is also only one stable OP, but it shows a large deviation from the reference which makes it unusable. In the region in-between (f_{r3}), two more operating points emerge, leading to a situation similar with the MCF. There are two stable OPs (③, ⑤) and one unstable in-between of them (④).

For a useful control system, only one stable OP is desirable. To accomplish this, the maximum input frequency should be limited. The useful frequency range can also be easily extended, using a higher gain in the control filter. Furthermore, the tuning range of the filter is limited anyway in a practical system.

C. Measurements

A PCF system was realised to validate the results. A first order parallel coupled filter with a varactor diode in the middle of the resonator was used. The phase sensitive detector was implemented as a singly balanced mixer comprising a Lange coupler, a matching network and a diode pair.

The filter is tunable from $2.2\,\mathrm{GHz}$ to $2.8\,\mathrm{GHz}$, the quiescent frequency $\omega_{0,0}$ was shifted to be in the middle at $2.5\,\mathrm{GHz}$ using a DC-offset. The system parameters k_f,

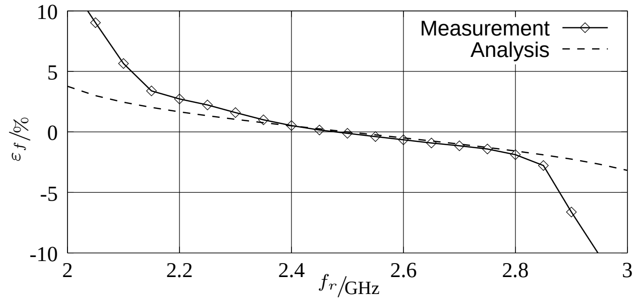

Fig. 7. Comparison of the relative frequency error between the analytical result and the measurement.

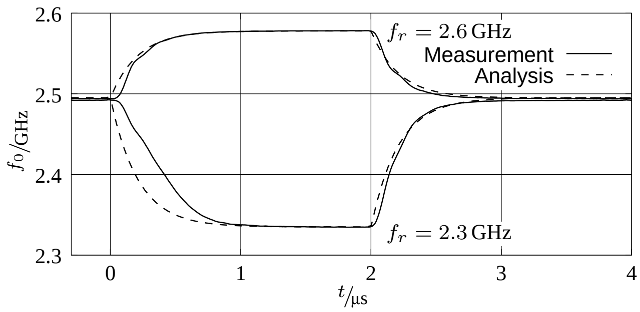

Fig. 8. Comparison of the settling behaviour between the measurement and a first order system. The reference frequency is switched from $2.5\,\mathrm{GHz}$ the indicated value.

$k_m \hat{u}_r^2$, Q_0, H_0 that were used in the previous analysis were derived at an input power level of $-8\,\mathrm{dBm}$ at $2.5\,\mathrm{GHz}$.

The control filter was designed for a DC-gain of $A = 100$ and a $3\,\mathrm{dB}$-cutoff at $125\,\mathrm{kHz}$. It was implemented with an operational amplifier.

Fig. 7 shows the relative frequency error

$$\varepsilon_f = \frac{f_r - f_0}{f_r} \tag{18}$$

for measurement and analysis. The deterioration above $2.8\,\mathrm{GHz}$ and below $2.2\,\mathrm{GHz}$ is due to the limited tuning range of the filter. The error could be reduced with a higher DC-gain in the control filter.

Since the linearised system is of first order, an exponential settling behaviour is expected. Fig. 8 compares the measurements that were done, switching between two sources of different frequencies, with the exponential settling of a first order system. The start and stop frequency were fitted to agree with the measurement, the time constant was derived from the linearised equation as $\tau = 211\,\mathrm{ns}$.

For small deviations from the OP ($f_r = 2.6\,\mathrm{GHz}$), measurement and analysis are in good agreement. For larger deviations (e.g. $f_r = 2.3\,\mathrm{GHz}$) the linear approximation is not accurate enough to describe the system.

IV. Conclusion

In this paper an automatic frequency control systems for tunable filters was analysed. The obtained results were demonstrated for a magnitude and for a phase sensitive detector. Measurements for a filter at microwave frequencies were presented that confirm the theoretical results. Due to its generality, the method might be easily applied to other types of detectors and control filters.

References

[1] Y. P. Tsividis and J. O. Voorman, Eds., *Integrated continuous-time filters*. IEEE press, New York, 1993.

[2] P. Katzin, B. Bedard, and Y. Ayasli, “Narrow-band MMIC filters with automatic tuning and Q-factor control,” in *IEEE MTT-S International Microwave Symposium Digest 93*, 1993, pp. 403–406.

[3] V. Aparin and P. Katzin, “Active GaAs MMIC band-pass filter with automatic frequency tuning and insertion loss control,” *IEEE Journal of Solid-State Circuits*, vol. 30, no. 10, pp. 1068–1073, 1995.

[4] S. Quintanel, H. Serhan, L. Billonnet, B. Jarry, and P. Guillon, “Theoretical and experimental analysis of automatic frequency control techniques for microwave active filters,” in *EuMC Conference Proceedings*, October 2000, pp. 47–50.

[5] A. J. Viterbi, *Principles of Coherent Communication*. McGraw-Hill, 1966.

[6] W. C. Lindsey, *Synchronisation Systems in Communication and Control*. Prentice-Hall, 1972.

[7] H. Meyr and G. Ascheid, *Synchronisation in Digital Communications*. John Wiley & Sons, 1990, vol. 1.

[8] J. van de Vegte, *Feedback Control Systems*. Prentice-Hall, 1986.